JOURNAL OF CATALYSIS 33, 219–232 (1974)

Surface Reduction and Support Interactions in the Water–Gas Shift Reaction Catalyzed by Europium Oxides

PHILIP N. ROSS, JR., AND W. NICHOLAS DELGASS

Department of Engineering and Applied Science, Yale University, New Haven, Connecticut 06520

Received September 10, 1973

The reaction $H_2 + CO_2 \rightleftarrows CO + H_2O$ has been studied at 500°C over bulk Eu_2O_3 and supported europium. A regenerative kinetic sequence with CO_2 poisoning fits the rate maximum as a function of P_{CO_2} for Eu_2O_3. A regenerative sequence for highly dispersed europium is supported by a strong correlation between the rate and the extent of $Eu^{3+} \rightarrow Eu^{2+}$ reduction in H_2 at 500°C shown by the Mössbauer effect. Comparison of data for Eu_2O_3 and supported Eu indicates that dispersion of europium on Al_2O_3 or SiO_2 alters both the nature of CO_2 chemisorption and the kinetic parameters. This is taken as the catalytic result of the strong Eu-support interactions shown in the Mössbauer spectra.

INTRODUCTION

Previous work (*1*) has established that some oxidation reactions over oxide catalysts proceed via a regenerative sequence in which the substance to be oxidized reacts with lattice oxygen of the catalyst surface and the surface oxygen content is restored by reaction of the catalyst with the oxidizing agent. Activation energies for such reactions have been correlated with the rate of heterogeneous oxygen exchange ($^{16}O_{lat} + 1/2\ ^{18}O_2 \rightarrow {}^{16}O^{18}O$) (*2*), which in turn has been found to be a direct measure of the surface cation–oxygen bond energy in transition metal oxides (*3*). Since the heterogeneous oxygen exchange rate over rare earth oxides is near that for transition metal oxides (*4*), rare earth oxides may be expected to have significant activity in oxidation reactions which proceed via a regenerative sequence. We have used europium catalysts to investigate this expectation for the water–gas shift reaction because the convenient Mössbauer parameters of ^{151}Eu provide a means for detailed catalyst characterization.

We reported earlier (*5*) that Eu^{3+} highly dispersed on η-Al_2O_3 and SiO_2 is significantly reduced to Eu^{2+} by H_2 and CO at temperatures from 400° to 500°C. The variation in extent of reduction of Eu/Al_2O_3 at 500°C in hydrogen was a nonlinear function of Eu loading, as shown in Fig. 1. In addition, changes in the Mössbauer parameters of various catalysts as a function of treatment indicated high Eu dispersion (except at 27% loading), strong interaction between Eu^{3+} and the support after initial dehydration, and reoxidation of supported Eu^{2+} by O_2 or CO_2 at room temperature and H_2O at 400°–500°C.

It is to be expected that when a cation is bound to the surface of an oxide support, its chemistry will be different from that on the surface of the pure oxide (*6*). This chemical difference will be accentuated when the added cation has different size or electronic structure compared to the support cations. To examine such support effects we have compared the catalytic and chemisorption behavior of bulk Eu_2O_3 to that for a series of supported catalysts. This paper presents a self-consistent analysis of chemisorption, kinetic, and Mössbauer data for all samples and shows that Eu-support interactions affect both the kinetics of the reverse water–gas shift reaction and the chemisorption of CO_2 over

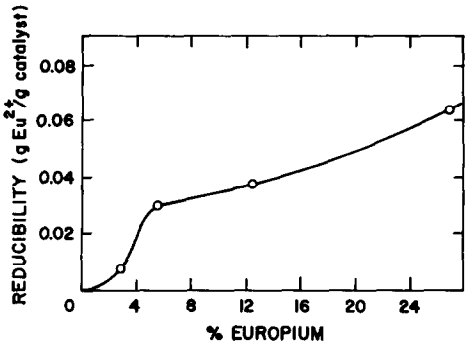

FIG. 1. Reducibility, from Mössbauer spectral area ratios after 6-hr reduction in H_2 at 500°C, for europium supported on alumina as a function of loading (Data from Ref. 5).

Eu-containing oxides. Furthermore, rates of the reaction over highly dispersed europium catalysts are found to correlate with the reducibility of Eu defined by the Mössbauer data in Fig. 1.

EXPERIMENTAL

Catalyst Preparation

Harshaw η-Al_2O_3 (Al-0102 P), 325 mesh and having a measured BET area of 130 m^2/g, and Cab-O-Sil silica M-5, having a measured BET area of 170 m^2/g, were used as supports. The supported europium was obtained by impregnation of supports at pH 7–7.5 with aqueous solution of the nitrate salt (Lindsay Rare Earths 99.9%) followed by air-drying for 12 hr at 140°C. The europium content was determined by X-ray fluorescence, and samples designated n Eu/support indicate *n* wt% europium.

Adsorption and Mössbauer Studies

The apparatus for observing the Mössbauer effect in europium was the same as that used previously (*5*) and is described in detail in (*7*). The vacuum and gas handling system, used for both treatment of Mössbauer samples and for adsorption studies, is depicted in Fig. 2a. The pumping system consisted of a Granville Phillips Series 244 2″ Cryosorb Cold Trap, an NRC HS2 oil diffusion pump with Dow 705 pump fluid, and a 5.6 CFM Welsh Duo-Seal roughing pump. The vacuum manifold was

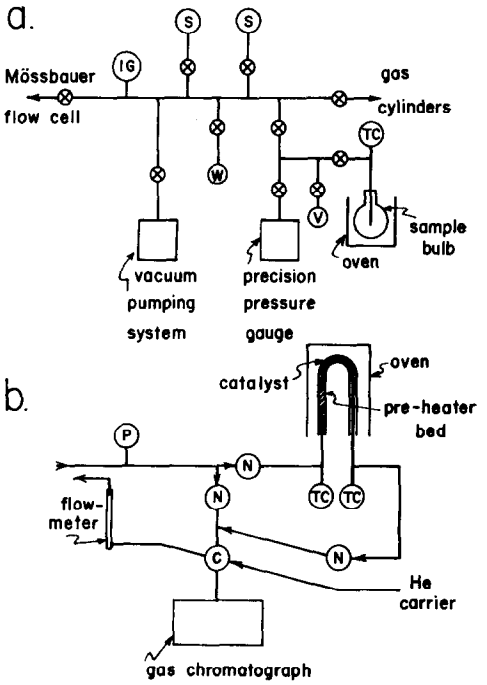

FIG. 2. Schematic of vacuum and gas handling system (a) and flow reactor (b): IG, Ionization gauge; S, gas storage bulb; ⊗, stopcock; TC, thermocouple leads; V, calibrated volume; W, H_2O storage flask; P, pressure gauge; N, needle valve; C, Carle 6-way sampling valve.

constructed entirely of Pyrex, using hollow bore vacuum stopcocks. Matheson Ultra High Purity grade hydrogen (99.999%, dew point −85°F), Matheson CP grade carbon monoxide (99.5%) and Matheson Research grade carbon dioxide (99.9999%) were stored in the gas storage bulbs and used without further purification. Water vapor could be introduced to the system by evaporation at 25°C from a 50-ml vacuum flask.

The adsorption cell was a small quartz bulb, attached to a graded Vycor to Kovar connector, sealed into a ¼ inch Swagelok Tee. A shielded chromel–alumel thermocouple was connected through the tee so that the tip of the thermocouple touched the powdered sample in the bulb. The standard pretreatment of the sample was to outgas at 550°C for 12 hr at 1×10^{-6} torr then cool in vacuum to the temperature of adsorption. To determine whether the

adsorption was reversible, the sample was outgassed 6 hr at the temperature of the adsorption and the adsorption repeated. Adsorption isotherms were calculated in the usual way from the pressure of known aliquots of gas exposed to the sample in a known volume.

Reaction Kinetics

A steady-state packed-bed flow reactor (Fig. 2b) was used to measure the initial rate of the reverse water–gas shift reaction ($H_2 + CO_2 \rightarrow CO + H_2O$) as a function of H_2 and CO_2 partial pressures. The gas delivery manifold provided accurate metering of H_2/CO_2 mixtures from 25:1 to 2:1 with a total flow generally less than 50 cc/min. The flow of H_2, CO, and He was metered directly from the cylinders by 150 mm Matheson rotometers with NRS high accuracy needle valves, and the CO_2 flow metered by a Matheson low flow flowmeter, a Whitey 22 RS4 micro-metering valve, and a Matheson 40L line regulator. H_2, CO, and CO_2 were the same grades used for adsorption. He was Matheson ultra high purity (99.999%). All gases were used without additional purification. The total flow rate through the catalyst bed was measured from the rate of rise of a soap-film in a burette. Chromel–alumel open junction thermocouples at each end of the catalyst bed indicated a temperature rise of less than 5°C. A Beckman GC-5 gas chromatograph provided analysis of both the feed and product streams. The sampling was by means of an He purged Carle sampling valve. Gas separation was accomplished with a 6-ft Poropak Q column operated isothermally at 30°C. Since H_2 peak areas could not be accurately evaluated because of the complicated nature of the thermal conductivity of H_2/He mixtures (*8*) and the H_2O peak suffered from extreme tailing, conversions were calculated from the CO/CO_2 area ratios.

The supported europium catalysts studied had all been previously reduced in H_2 at 500°C and the extent of reduction measured in Mössbauer flow cell. The sample wafers were then ground, sieved to 40/100 mesh, diluted with a 3:1 weight ratio of similarly sized glass beads, and pretreated with H_2 at 500°C for 12 hr. Reactor tubes of pure oxide catalysts were prepared similarly from pressed wafers and were also pretreated in H_2 at 500°C for 12 hr. All reactor tubes had a gas preheating section of 40/50 mesh glass beads. Kinetic experiments were begun by metering CO_2 into the H_2 stream so that the catalyst was always in a reducing environment.

Results

Mössbauer Studies

Mössbauer results obtained previously (*5*) for supported europium have been summarized in the introduction. New results are summarized here. To further investigate irreversible changes in the bonding of Eu^{3+} to the support after initial dehydration at high temperatures, effective Debye temperatures, θ_D, of various catalysts were obtained for fresh and heated samples. Ratios of spectral areas at 25°C and −196°C, obtained using a metal liquid nitrogen Dewar with the sample in vacuo, provided the data for iterative calculations (*9*) of the θ_D values presented in Table 1. These values indicate strong Eu^{3+}-support interactions after drying samples at 420°C. The low θ_D for 27 Eu/Al_2O_3 agrees with X-ray observation (*5*) of Eu_2O_3 particles in this particular material. While the Debye theory is not expected to be accurate for these composite solids, it is interesting that the high values of θ_D are contrary to expectations for a heavy, Eu^{3+} impurity in an

TABLE 1
APPARENT DEBYE TEMPERATURES, θ_D FROM MÖSSBAUER DATA

Sample	Treatment (°C)	θ_D (°K)	Ref.
10.5 Eu/SiO_2	Evac 25	208	This work
10.5 Eu/SiO_2	Evac 420	373	This work
5.5 Eu/Al_2O_3	Evac 25	223	This work
5.5 Eu/Al_2O_3	Evac 420	515	This work
27 Eu/Al_2O_3	Evac 420	272	This work
Eu_2O_3	—	189	(*10*)
SiO_2	—	470	(*11*)
Al_2O_3	—	495	(*12*)

TABLE 2
EFFECT OF ADSORPTION AT 25°C ON MÖSSBAUER PARAMETERS OF 5.5% Eu/Al_2O_3

Sequential treatment	Isomer shift (mm/sec)	Line width (mm/sec)	Relative area
Fresh	−0.55	3.0	1.0
NH_3, 340 torr	−0.40	3.2	1.25
EVAC at 420°C	−0.32	4.5	3.0
NH_3, 340 torr	−0.27	3.9	2.75
Fresh	−0.55	3.0	1.0
CO_2, 340 torr	−0.65	3.0	1.4
EVAC at 420°C	−0.33	5.2	3.8
CO_2, 340 torr	−0.38	4.2	3.1

Al_2O_3 or SiO_2 lattice (*13*) and to the decrease in θ_D expected for surface atoms (*14*). Thus these results indicate increased Eu–O force constants and a strong Eu–support interaction.

The 5.5 Eu/Al_2O_3 material was also used in further adsorption studies. Table 2 shows significant changes in Mössbauer parameters as a result of adsorption. The decrease in *IS* caused by CO_2 adsorption suggests increased ionic character of the Eu^{3+} bonding and a trend toward the value of *IS* = −0.8 mm/sec for $Eu_2(CO_3)_3$ (*15*). The increase in *IS* on NH_3 adsorption reflects a strong interaction between NH_3 and Eu^{3+} (or possibly Eu^{3+}–OH) and suggests an increase in covalency or a decrease in Eu–O bond distance on adsorption (*16*).

It is important to point out that these new results corroborate the conclusion that on all the catalysts prepared but 27 Eu/Al_2O_3, the europium is highly dispersed.

Volumetric Chemisorption

Since it is not possible to study adsorption of gases on bulk, crystalline Eu_2O_3 by Mössbauer spectroscopy, the more conventional technique of volumetric chemisorption was used to determine how H_2, CO_2, and H_2O interact with Eu_2O_3 at reaction conditions. Studies of chemisorption of CO_2 on supported europium were also included to facilitate further comparison of the surface chemistry of supported and unsupported oxides.

TABLE 3
APPARENT UPTAKE OF HYDROGEN BY Eu_2O_3 AT 500°C AND P_{H_2} = 290 TORR[a]

Doses of H_2	1	2	3	4
Apparent uptake (μmoles/m^2)	2.60	1.15	0.75	0.38

[a] Sample evacuated for 2 hr at 500°C between doses.

While bulk reduction of $Eu_2O_3 \rightarrow EuO$ by hydrogen is negligible at temperatures below 1200°C, the chemical behavior of the surface is not governed by the same thermodynamic limits. Fresh Eu_2O_3 which had been heated to 550°C in vacuum for 12 hours did not adsorb a measurable ($<10^{-8}$ moles/m^2) quantity of O_2 at 500°C and a pressure of 300 torr, indicating that the stoichiometry of the oxide surface was not altered by heating to high temperature in vacuum. At 25°C, there was no measurable uptake of H_2 following the standard outgassing pretreatment. At 500°C, however, a considerable uptake of H_2 was observed. Table 3 shows a decrease in the "apparent" uptake of H_2 at a constant pressure of 290 torr at 500°C as a function of the number of sequential doses of H_2 with intervening sample evacuation for 2 hr at 500°C. The association of this behavior with surface reduction was reinforced when it was found that 1.59 μmoles/m^2 of O_2 were taken up at 25°C and 300 torr pressure after evacuation for 2 hr at 500°C following four doses of a fresh Eu_2O_3 surface with H_2 at 290 torr and 500°C. The extent of reduction is equivalent to 3.84×10^{18} atoms Eu^{3+} reduced/m^2 of Eu_2O_3 surface. This corresponds to approximately 40% of a europium monolayer reduced (assuming 1×10^{19} surface Eu/m^2) or to 0.012 g of europium ions reduced per gram of Eu_2O_3 and is in line with the value of 0.0154 g of europium ions reduced per gram of Eu_2O_3 reported for reduction in H_2 at 650°C (*17*).

Of course, surface reduction can be observed by H_2 uptake only if the product H_2O is chemisorbed. Water adsorption isotherms for Eu_2O_3, pretreated by heating in vacuum at 550°C, showed a saturation

uptake at 25°C of about 9 μmoles/m^2 including about 1.5 μmoles/m^2 adsorbed irreversibly. At 500°C, adsorption of H_2O was reversible and the saturation coverage, 2 μmoles/m^2, was nearly equal to that irreversibly adsorbed at 25°C. Thus, H_2O adsorption capacity was sufficient to accommodate product water and decreasing H_2 uptake on repeated dosing is taken to indicate surface reduction. Irreversible adsorption of water at room temperature may indicate rehydroxylation of a freshly outgassed surface.

Adsorption of CO_2 was studied on both Eu_2O_3 and η-Al_2O_3. In the temperature region 25°–100°C, alumina adsorbed CO_2 reversibly with a heat of adsorption which varied with coverage from 13–20 kcal/gmole and a saturation coverage of 4 μmoles/m^2. At 25°C saturation coverage of Eu_2O_3 was 6 μmole/m^2 but in this case the adsorption was strongly irreversible. Seventy percent of the adsorbed CO_2 was not desorbed after outgassing for 6 hr at 25°C. CO_2 was still strongly adsorbed on Eu_2O_3 at 450–500°C, as shown in Fig. 3 and had a complex isotherm. The total amount of irreversible adsorption at 500°C remained high, about 50% of the total uptake, and it was found that outgassing at 600–650°C was necessary to remove the last traces of adsorbed CO_2. For each isotherm shown in Fig. 3, the Eu_2O_3 had been preheated in vacuum at 650°C for 12 hr. In contrast, adsorption of CO_2 on η-Al_2O_3 at 500°C was reversible with a heat of adsorption which varied with coverage from 17 to 25 kcal/gmole (calculated from data at T = 455°–510°C). The isotherm is also shown in Fig. 3.

The shape of the CO_2 isotherm on Eu_2O_3 at 485°–507°C indicates at least two different kinds of adsorbed species, one corresponding to the sharp uptake at 0–40 Torr, the other to the steady, nearly linear uptake of CO_2 at higher pressure. These two species are postulated to occupy different types of sites. At the maximum pressure measurable with the Texas Instruments pressure gauge, 800 Torr, the total uptake at 450°–500°C approached the total uptake at 25°C, 6 μmoles/m^2, or 36×10^{17} molecules/m^2. Rare earth oxides are known to form very stable surface carbonates (*18*) and it seems likely that the irreversibly adsorbed CO_2 corresponds to such a species. Following CO_2 adsorption at 507°C and outgassing in vacuum at the same temperature, the re-adsorption of CO_2, shown in Fig. 3, produced an isotherm like that observed for η-Al_2O_3 with saturation of the surface at $P_{CO_2} > 80$ Torr. Conclusions based on readsorption are tentative since the surface may be more car-

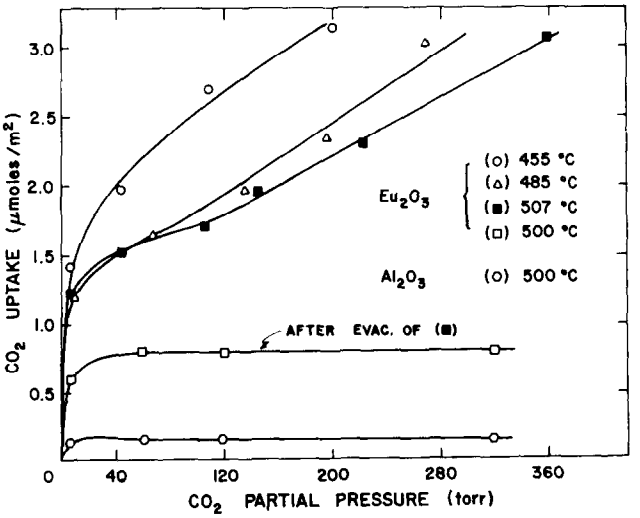

FIG. 3. Adsorption of CO_2 on Eu_2O_3 and Al_2O_3 at high temperature.

bonate than oxide, but if the re-adsorption is accepted as characteristic of reversible adsorption on the oxide surface, then the sharp rise in the adsorption at $P_{CO_2} < 40$ Torr may represent the formation of a CO_2 adsorption complex while the nearly linear portion of the adsorption for $P_{CO_2} > 120$ Torr represents formation of the surface carbonate.

From the Mössbauer experiments, it is known that CO_2 adsorption on supported europium at 25°C produced a change in isomer shift indicative of a strong interaction between CO_2 and the europium ion. Since the direction of the isomer shift change indicated the possibility of carbonate formation, it is of interest to compare CO_2 adsorption on supported europium to that on Eu_2O_3. Unfortunately, CO_2 uptake on alumina at 25°C was too extensive to allow differentiation of adsorption on the europium from that on alumina. At high temperature, however, the adsorption on alumina was greatly reduced and volumetric measurement of CO_2 chemisorption on supported Eu was possible. With the assumption of 100% dispersion of the europium ions at a density of 10^{19} Eu^{3+}/m^2 and an Al_2O_3 surface area of 130 m^2/g, 0.45 g of 5.5 Eu/Al_2O_3 would have an available alumina surface area of 45.5 m^2 and an effective europium area of 10 m^2. Figure 4 shows the adsorption of CO_2 on 0.45 g of 5.5 Eu/Al_2O_3 at 502°C together with the calculated amount of adsorption for 45.5 m^2 of η-Al_2O_3 and 10 m^2 of Eu_2O_3. It is clear that the adsorption on supported Eu was similar to that on pure alumina and far from the isotherm for the equivalent area of Eu_2O_3. In addition, the adsorption on supported europium was reversible with a heat of adsorption which varied with coverage from 15 to 23 kcal/gmole (calculated from data at $T = 455°$–$510°C$), about the same as that measured for η-Al_2O_3. Even if the dispersion were as low as 20% and the effective Eu_2O_3 area 2 m^2, the sum of expected adsorption on Eu_2O_3 and η-Al_2O_3 would lie considerably above the observed isotherm. Furthermore, the facts that the adsorption was entirely reversible and that saturation of the surface occurred at $P_{CO_2} \sim$ 150 torr both indicate that the nature of the adsorption of CO_2 on 5.5 Eu/Al_2O_3 at high temperature was not like that observed on Eu_2O_3. To determine whether the europium on the surface had any effect on the adsorption, the adsorption on 0.6 g of 12.5 Eu/Al_2O_3 was measured. Again assuming 100% dispersion of europium ions, 0.6 g of 12.5 Eu/Al_2O_3 would have the same available alumina area, three times the effective europium area, and 30% more total area than the 5.5 Eu/Al_2O_3 sample above. As the

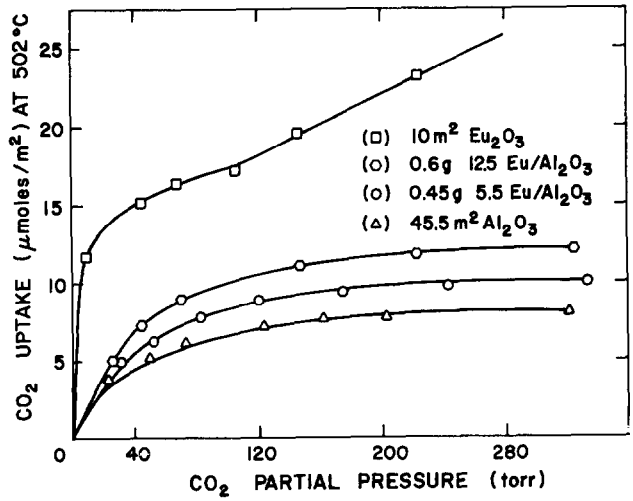

FIG. 4. CO_2 adsorption on supported europium at 502°C. (◯) and (○) as measured; (□) and (△) calculated from data in Fig. 3.

isotherm of Fig. 4 indicates, the uptake on 0.6 g of 12.5 Eu/Al_2O_3 was approximately 30% greater than (rather than the same as or three times greater than) the uptake on 0.45 g of 5.5 Eu/Al_2O_3. Thus, supported europium appears to adsorb CO_2 to the same extent at high temperature as the surface of the alumina support.

Although the uptake/m^2 of CO_2 on SiO_2 at 25°C was much less than that for alumina, the nature of the adsorption on SiO_2 at high temperature was found to be nearly identical to that on η-Al_2O_3 in both amount and heat of adsorption. The adsorption of CO_2 at 505°C on 0.36 g of 10.5/SiO_2, which had the same *total* surface area as 0.45 g of 5.5 Eu/Al_2O_3, produced an isotherm nearly identical to the one observed for 0.45 g of 5.5 Eu/Al_2O_3 at 502°C.

Kinetics of the Reverse of the Water–Gas Shift Reaction

The standard experimental procedures indicated the absence of either bulk or intraparticle diffusion limitations for all kinetic experiments (7). Within the experimental reproducibility of ±10%, rates of reaction were constant for a doubling of flow velocity at constant space velocity and for a threefold change in log mean particle size. Since, as shown below, specific rates were identical for silica and alumina supported Eu and since cabosil has no micropore structure, intraparticle diffusion limitations were deemed unlikely. Inhibition of the reaction rate by products was found to be negligible for $P_{CO} < 12$ Torr and $P_{H_2O} < 23$ Torr at the reactor inlet. Thus for the reaction conditions of this study, the reactor was treated as differential for conversions of 3–7%. Two types of kinetic data were obtained.

The first type was the initial rate of reaction in binary mixtures of H_2 and CO_2, no diluent added. Data for the bulk oxides Eu_2O_3, η-Al_2O_3, and La_2O_3 are illustrated in Fig. 5 while results for some supported oxides (corrected for the contribution of the support) are shown in Figs. 6 and 7. The rate over SiO_2 was observed to be at least an order of magnitude smaller than any reported above. Its activity can, therefore, be considered negligible. As seen in Fig. 5, the alumina support must have contributed to the observed rate for the Eu/Al_2O_3 catalysts. Corrections for the support contribution to the rate were calculated assum-

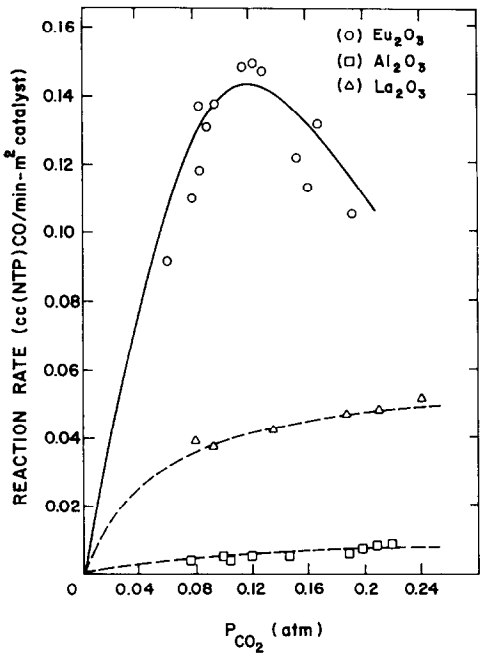

FIG. 5. Initial rate of the reverse of the water–gas shift reaction in H_2/CO_2 binary mixtures at 505°C and 1.05 atm total pressure. Full line corresponds to fitted parameters in Table 7.

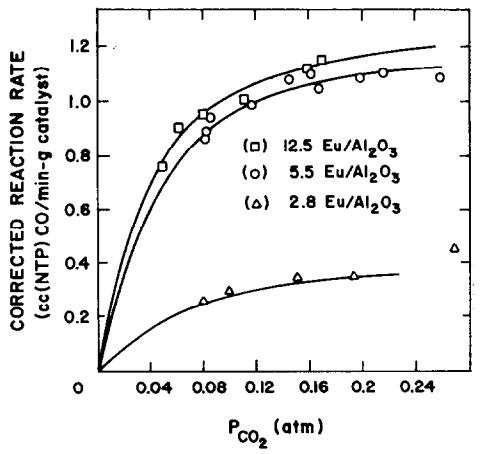

FIG. 6. Corrected reaction rate in H_2/CO_2 binary mixtures for europium supported on alumina at 505°C and 1.05 atm total pressure. Curves correspond to fitted parameters in Table 7.

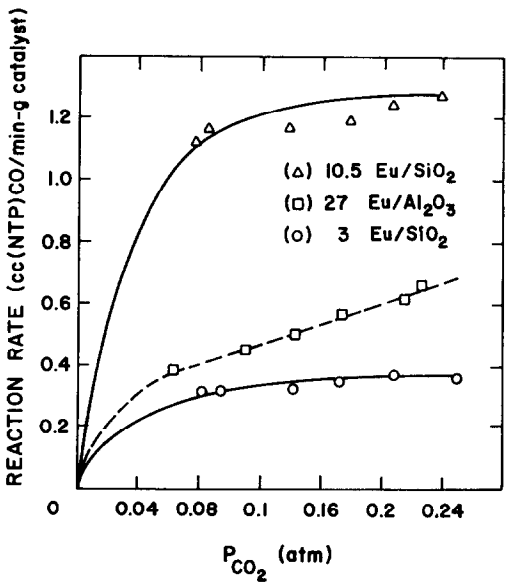

FIG. 7. Reaction rate in H_2/CO_2 binary mixtures for supported europium at 505°C and 1.05 atm total pressure. Full lines correspond to fitted parameters in Table 7.

ing 100% dispersion of the europium on the alumina surface and using the rate/m² obtained for pure η-Al_2O_3 at identical conditions. Although the assumption of 100% dispersion is extreme, the Mössbauer results have shown the dispersion to be high, and the corrected rates have a CO_2 partial pressure dependence qualitatively similar to that observed for europium on silica (Fig. 7) as expected from the similarity of the chemical characterization of Eu/SiO_2 and Eu/Al_2O_3.

The second type of kinetic data was the order of the reaction in CO_2 and H_2 obtained in the usual way by varying one partial pressure while holding the other constant and introducing a diluent, in this case He. The orders of reaction at 505°C and the pressures for which they apply are given in Table 4.

It is obvious from Fig. 5 that the kinetics of the reaction over Eu_2O_3 are clearly different from those observed for supported europium and the other oxides studied. To compare the relative activities of the pure oxides, Table 5 presents reaction rates at a single set of conditions corresponding to values of P_{H_2} and P_{CO_2} on the nearly linear region of the Eu_2O_3 curve, well away from the maximum rate. At these conditions, Eu_2O_3 was 40 times as active as η-Al_2O_3 and nearly 4 times as active as La_2O_3. The apparent activation energy, calculated from the temperature dependence of the reaction rate at the specified partial pressures, was significantly lower for Eu_2O_3 than La_2O_3 or η-Al_2O_3.

The apparent activation energy of the reaction over Eu_2O_3 increased significantly (and reversibly) as the CO_2 level in the feed increased to the other side of the maximum in the rate. Table 6 compares the activation energies (calculated from data corresponding to T = 495°–530°C) for the reaction over Eu_2O_3 and over the supported oxides at P_{H_2}, P_{CO_2} values on each side of the maximum in the rate for Eu_2O_3. The activation energies for the supported oxides showed almost no change with P_{CO_2} and were uniformly lower than for Eu_2O_3. The higher activation energy at higher P_{CO_2} for Eu_2O_3 implies that as the temperature is raised the maximum in the rate would become less sharp and would eventually dis-

TABLE 4
ORDERS OF REACTION IN H_2 AND CO_2 AT 505°C

Catalyst	Order	Conditions (atm)
Eu_2O_3	$r = kP_{H_2}^{0.5}P_{CO_2}^{0.9}$	$0.05 < P_{CO_2} < 0.125$ $0.55 < P_{H_2} < 0.97$
	$r = kP_{H_2}P_{CO_2}^{-0.8}$	$0.15 < P_{CO_2} < 0.32$ $0.75 < P_{H_2} < 0.96$
$3\ Eu/SiO_2$	$r = kP_{H_2}P_{CO_2}^{0.2}$	$0.06 < P_{CO_2} < 0.32$ $0.60 < P_{H_2} < 0.96$
$5.5\ Eu/Al_2O_3$	$r = kP_{H_2}P_{CO_2}^{0.3}$	$0.05 < P_{CO_2} < 0.32$ $0.60 < P_{H_2} < 0.96$

TABLE 5
ACTIVATION ENERGY AND INITIAL RATE OF REACTION FOR BULK OXIDES[a]

Catalyst	BET area (m^2)	Reaction rate [cc(NTP)CO/min-m^2]	E_{act} (kcal/gmole)
η-Al_2O_3	130	3.29×10^{-3}	40
SiO_2	170	$\ll 10^{-3}$	—
Eu_2O_3	12	1.22×10^{-1}	27
La_2O_3	6	3.87×10^{-2}	32

[a] T = 505°C; P_{CO_2} = 0.08 atm; P_{H_2} = 0.97 atm.

TABLE 6
APPARENT ACTIVATION ENERGIES

Catalyst	E_{act} for P_{CO_2} = 0.08, P_{H_2} = 0.97 (kcal/gmole)	E_{act} for P_{CO_2} = 0.20, P_{H_2} = 0.85 (kcal/gmole)
Eu_2O_3	27	36
2.8 Eu/Al_2O_3	20	20
5.5 Eu/Al_2O_3	19	20
12.5 Eu/Al_2O_3	20	22
27 Eu/Al_2O_3	26	28
3 Eu/SiO_2	22	22

appear. The highest temperature used in this work was 526°C, for which the maximum was only slightly broadened from that at 500°C.

The kinetics of the reverse water–gas shift reaction catalyzed by Co_3O_4 were also measured. Co_3O_4 is known to catalyze most oxidation–reduction reactions at relatively high temperature by a regenerative sequence (*19*), but also forms a relatively stable surface carbonate in the presence of CO_2 (*20*). Thus, it provides a convenient experimental comparison with the kinetic results for Eu_2O_3. On Co_3O_4, decomposition of the surface carbonate occurs at much lower temperature (375°–400°C) (*20*) than for the rare earth oxides. Thus, to include the complication of carbonate formation, initial rates were measured at 250°–350°C, the temperature region in which Co_3O_4 is used commercially as the active component of a "low temperature" shift catalyst. The kinetics for Co_3O_4 showed many of the features observed for Eu_2O_3. The initial rate passed through a broad maximum at P_{CO_2} = 110 Torr (0.14 atm) and the activation energy was found to increase with increasing CO_2 partial pressure, from 6 kcal/gmole at P_{CO_2} = 0.08 atm, P_{H_2} = 0.97 atm, to 12 kcal/gmole at P_{CO_2} = 0.24 atm, P_{H_2} = 0.80 atm.

DISCUSSION

Kinetics of the Reverse of the Water–Gas Shift Reaction over Eu_2O_3

In order to discuss the kinetics we have analyzed the data in terms of an oxidation–reduction sequence of kinetic steps. It will be shown that this approach produces a straightforward model of the kinetics which is consistent with all the data available. Although it appears that surface oxidation–reduction can occur on all the catalysts, it should be emphasized that the kinetic analysis does not prove that the oxidation-reduction sites are the active sites or that the kinetic sequence presented is the only valid one. The self-consistent picture of the catalytic activity rendered by this model does, however, provide a useful basis for comparison of the catalytic behavior of Eu_2O_3 to that of supported europium.

The Eu_2O_3 data is considered first because the sharp maximum in the rate as a function of CO_2 partial pressure (see Fig. 5) is more difficult to fit than the smooth rate functions associated with supported Eu (Figs. 6 and 7) and thus requires the highest complexity of the model. In the following sequence of steps for $CO_2 + H_2 \rightarrow CO + H_2O$ over Eu_2O_3 two different types of CO_2 chemisorption sites were found necessary for a good fit to the maximum and are also consistent with the chemisorption data:

$$CO_2 + (S) \underset{k-1}{\overset{k_1}{\rightleftarrows}} (CO_2 - S) \quad (1)$$

$$H_2 + (\boxdot) \xrightarrow{k_2} H_2O + (\square) \quad (2)$$

$$CO_2 + (\boxdot) \underset{k-3}{\overset{k_3}{\rightleftarrows}} (CO_3^*) \quad (3)$$

$$(CO_2 - S) + (\square) \xrightarrow{k_4} CO + (\boxdot) + (S) \quad (4)$$

where ($\boxdot$) is a lattice oxide ion site, ($\square$)

is a lattice oxide ion vacancy, and (S) is a general surface site for CO_2 adsorption in the weakly bound, reversible state. In step (3) it is assumed, following Artamov and Sazonov (*18*), that strongly adsorbed CO_2 yields a carbonate-like species formed by adsorption of CO_2 on an active lattice oxide ion, which is then poisoned. Assuming further that (CO_3*) and ($CO_2 - S$) do not compete for the same sites, that step [1] is in quasiequilibrium ($k_4\square/k_{-1} \ll 1$), that S is the total number of general CO_2 adsorption sites and L is the total number of oxidation–reduction sites, then, at steady-state, this sequence yields Eq. (5) for the rate:

$$-dP_{CO_2}/dt = \frac{\alpha\beta P_{H_2}P_{CO_2}}{\alpha P_{H_2}(1 + K_1P_{CO_2}) + \beta P_{CO_2}(1 + K_3P_{CO_2})} \quad (5)$$

where $K_1 = k_1/k_{-1}$, $K_3 = k_3/k_{-3}$, $\alpha = Lk_2$, and $\beta = K_1S\,k_4\,L$.

When the full eight-parameter representation of Eq. (5) was used to fit kinetic data for Eu_2O_3 at three different temperatures, a convergent fit could not be found by the SHARE program GAUSHAUS, described by Weiner (*21*). Since the program indicated that K_1 (of order 1) was not a correlating parameter, Eq. (5) was rewritten as

$$-dP_{CO_2}/dt = \frac{\alpha\beta P_{H_2}P_{CO_2}}{\alpha P_{H_2} + \beta P_{CO_2} + \beta K_3 P_{CO_2}^2} \quad (6)$$

assuming $K_1P_{CO_2} \ll 1$. Using this equation, 27 data points taken at 505°, 515°, and 526°C were fit simultaneously to produce the parameters in Table 7 and the solid line through the data in Fig. 5. The entropy of adsorption, −22 e.u., for K_3 is in accord with the limits outlined by Boudart, Mears, and Vannice (*22*). This procedure produced poor fits (maxima too broad) when K_3 was constrained to be equal to zero or when the classical Langmuir-Hinshelwood rate expression for surface reaction between adsorbed H_2 and adsorbed CO_2 was used.

As required, Eq. (6) yields the correct limiting behavior. At very low CO_2 pressure

$$-dP_{CO_2}/dt = \beta P_{CO_2}, \quad (7)$$

while at high CO_2 pressure the limiting form is

$$-dP_{CO_2}/dt = \alpha(K_3)^{-1}P_{H_2}P_{CO_2}^{-1}. \quad (8)$$

Since one may expect the activation energy for reduction to be higher than that for oxidation (19) and $|\Delta H_{ads}|$ for K_3 to be greater than or equal to that for K_1, the apparent activation energy of the term β should be lower than that of αK_3^{-1}. In this way the qualitative trend of the data toward increasing apparent activation energy as the CO_2 partial pressure is increased is also explained by Eq. (6).

Comparison to Co_3O_4 can be made qualitatively. The maximum in the rate over Co_3O_4 was observed at about the same

TABLE 7

KINETIC PARAMETERS FOR SUPPORTED Eu AND Eu_2O_3 AT 505°C, TEMPERATURE COEFFICIENTS IN kcal/gmole

Catalyst	α cc (NTP) / min-gcat-atm	β cc (NTP) / min-gcat-atm	K_3 atm^{-1}
Eu_2O_3	16.6 (E_a = 15)	20.6 (E_a = 8)	35 (ΔH = −22)
3 Eu/SiO_2	0.520	10.1	
10.5 Eu/SiO_2	1.91	37.0	
2.8 Eu/Al_2O_3	0.471	6.13	
5.5 Eu/Al_2O_3	1.79	23.3	
12.5 Eu/Al_2O_3	1.88	24.5	

CO_2 partial pressure as that for Eu_2O_3. At low P_{CO_2}, the rate approached first-order dependence on CO_2 and the activation energy at $P_{CO_2} = 0.06$ atm was 6 kcal/gmole. On the high P_{CO_2} side of the maximum the decrease in rate was not as sharp for Co_3O_4 as for Eu_2O_3, but at $P_{CO_2} = 0.24$ atm the activation energy had doubled to 12 kcal/gmole, following the trend observed for Eu_2O_3 and by Mamedov *et al.* (*19*) for oxidation of H_2 over Co_3O_4. They report the activation energy for oxidation of the reduced surface as 5 kcal/gmole and that for the reduction of the oxidized surface at 16 kcal/gmole. It appears from the breadth of the rate maximum, however, that Co_3O_4 is less strongly affected by CO_2 poisoning than is Eu_2O_3.

Poisoning by CO_2 appears to be weaker still over La_2O_3, as shown by the lack of a maximum in the La_2O_3 data in Fig. 5. It is also interesting to note that the rate of the reverse of the water–gas shift reaction is significantly lower over La_2O_3 than Eu_2O_3, in accord with the more ready reducibility of the latter oxide.

Kinetics of the Reverse of the Water–Gas Shift Reaction over Supported Europium

It is apparent from the chemisorption data on supported europium and from the lack of inverse dependence of the rate on CO_2 pressure that the strong CO_2 chemisorption step [Eq. (3)] need not be included in this sequence of steps. While the kinetics over all supported Eu catalysts (except 27 Eu/Al_2O_3) appear to be similar, the near zero-order dependence of the rates on P_{CO_2} makes differentiation of various kinetic sequences impossible. In the following discussion, steps (1), (2), and (4) are adopted to describe the kinetics of $CO_2 + H_2 \rightarrow CO + H_2O$ over supported europium. Justification for this approach is developed by drawing on surface chemical properties elucidated by the Mössbauer effect to correlate the rate data. Use of this model also permits an interesting comparison of the catalytic behavior of bulk and supported europium oxides.

The general rate expression (5) yields expression (9) for the rate over supported europium when $K_3 = 0$ and $K_1\alpha/\beta \ll 1$.

$$-dP_{CO_2}/dt = \frac{\alpha\beta P_{H_2}P_{CO_2}}{\alpha P_{H_2} + \beta P_{CO_2}} \qquad (9)$$

A zero value of K_3 is just a statement of the lack of strong chemisorption on these materials. That $K_1\ \alpha \ll \beta$ is strongly supported by the Mössbauer results that prereduced 5.5 Eu/Al_2O_3 is rapidly reoxidized by CO_2 at room temperature while Eu^{3+}/Al_2O_3 is reduced by hydrogen only at temperatures above 420°C. Table 7 shows the result of fitting Eq. (9) to the corrected supported Eu kinetic data taken at 505°C. Good fits and consistent parameters were also obtained by similar fits to data on 5.5 Eu/Al_2O_3 at 475°C and 530°C. The values of α in Table 7 provide a good basis for discussion because in the region of low CO_2 order of reaction which applies the apparent rate constant is nearly equal to α.

Correlation of Rate with Reducibility Shown by the Mössbauer Effect

Although, as shown in Table 6, the activation energies for supported catalysts with Eu loadings $\leq 12.5\%$ are nearly constant, the corresponding α values in Table 7 show wide variation. This spread in α is not surprising because values are reported per gram of catalyst and no attempt has been made to account for changes in the value of L, the number of oxidation–reduction sites. A narrowing of the α spread should be expected if values are calculated per gram of europium in the catalyst. It is clear that this normalization is not sufficient, however, since 5.5 Eu/Al_2O_3 and 12.5 Eu/Al_2O_3 have nearly the same α per gram of catalyst but more than a factor of two difference in europium content. If, on the other hand, α' values are calculated per gram of reducible europium, as observed in Mössbauer spectra of catalysts reduced for 6 hr in H_2 at 500°C, a nearly constant set of α' values is produced (see Table 8). The correlation of the rate data by the reducibility of Eu is given in Fig. 8, which shows reaction rate per gram of reducible Eu at $P_{CO_2} = 0.08$ atm and $P_{H_2} = 0.97$ atm as a function of Eu loading. The constancy of this normalized rate for several catalysts

TABLE 8
NORMALIZATION OF KINETIC PARAMETERS BY REDUCIBILITY

Catalyst	L' $\left(\frac{\text{g reducible Eu}}{\text{g catalyst}}\right)$	α' $\left(\frac{\text{cc (NTP)}}{\text{min-g reducible Eu-atm}}\right)$	β' $\left(\frac{\text{cc (NTP)}}{\text{min-g reducible Eu-atm}}\right)$
3 Eu/SiO_2	0.013	40	775
10.5 Eu/SiO_2	0.044	43	835
2.8 Eu/Al_2O_3	0.0076	62	807
5.5 Eu/Al_2O_3	0.030	59	768
12.5 Eu/Al_2O_3	0.038	50	653
Eu_2O_3	0.012	1383	1717

suggests that the number of active sites is indeed related to the reducibility of the europium. It should be pointed out that since the greatest reducibility was not observed at the lowest Eu loading, where dispersion should be highest, it is unlikely that reducibility is simply a measure of surface area. While it is equally unlikely that the number of Eu^{3+} ions reduced to Eu^{2+} after 6 hr gives an accurate count of the number of oxidation–reduction sites, L, Fig. 8 does give strong support for the use of the regenerative sequence to describe the kinetics over supported europium.

Figure 8 also shows that the correlation holds only for europium in high dispersion. The 27 Eu/Al_2O_3 sample represents approximately monolayer coverage of Al_2O_3 by Eu. At this high loading, X-ray diffraction showed the presence of 400 Å particles of europium oxide. The high activation

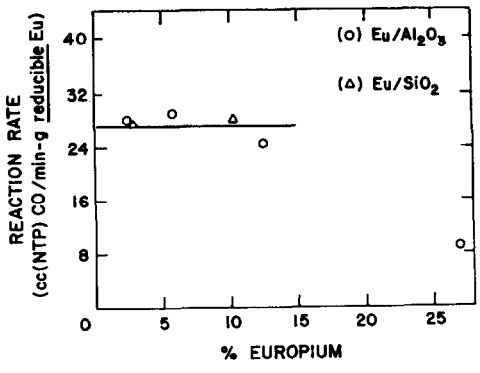

FIG. 8. Reaction rate at $P_{H_2} = 0.97$ atm and $P_{CO_2} = 0.08$ atm over supported europium normalized by the reducibility.

energies in Table 6 and lower effective Debye temperature in Table 1 support the assumption that the dispersion of this sample was low. Thus, the low value of the data point for the 27% sample in Fig. 8 suggests that all the reducible europium was not accessible to the reactants. This is consistent with the properties of the sample discussed above if one assumes a range of europium oxide particle sizes, with some particles small enough to be reduced but large enough to have a dispersion significantly less than one.

Comparison of Eu_2O_3 and Supported Eu

The success of the correlation in Fig. 8 suggests that the kinetic data for Eu_2O_3 should also be scaled to surface reducibility. This was done using the value of 0.012 g reducible Eu per gram of Eu_2O_3 from the oxygen back-titration measurement of surface reduction in H_2 at 500°C. The result is included in Table 8. If α' is taken as an effective rate constant for surface reduction and β' as an effective rate constant for surface oxidation, Table 8 shows that oxidation overpowers reduction on the supported Eu catalysts but that oxidation and reduction are nearly balanced on Eu_2O_3. Furthermore, comparison of Eu_2O_3 and supported Eu indicates that the rate constant for reduction is significantly lower on supported Eu. While β' is somewhat higher on Eu_2O_3 than supported Eu, chemisorption data showed that S is approximately five times higher for Eu_2O_3. Thus if the K_1 values are assumed to be similar, the in-

trinsic rate constant for surface reoxidation, k_4, would be higher for supported europium than for Eu_2O_3.

This analysis suggests an interesting contrast between the two types of catalysts. The apparent rate constants indicate a favorable balance between surface oxidation and reduction on Eu_2O_3, but as a stoichiometric mixture of H_2 and CO_2 is approached, strong CO_2 chemisorption poisons the surface and lowers the rate. When europium is highly dispersed on Al_2O_3 or SiO_2 it loses its ability to adsorb CO_2 strongly and is no longer poisoned by CO_2. Unfortunately dispersion also alters the oxidation–reduction balance by lowering the rate constant for reduction with respect to that for reoxidation.

A check on the consistency of this analysis can be provided by *in situ* Mössbauer examination of the supported catalysts during reaction. Values for the state of reduction of the surface *in situ* as a function of the ratio P_{H_2}/P_{CO_2} can then be compared to values predicted for $\square/L$ by the observed kinetic parameters. Preliminary experiments of this kind by L. Y. Chen in this laboratory have shown that the state of reduction of the surface of 5.5 Eu/Al_2O_3 at 500°C in a flowing mixture of CO_2 and H_2 is indeed a function of the P_{H_2}/P_{CO_2} ratio. They also suggest, however, that after exposure of this catalyst to CO_2 at a partial pressure of 400 torr at 500°C, some of the Eu^{3+} ions lose their reducibility. This complication of the Eu surface chemistry and the question of whether the number of kinetically important sites, L, is a measurable fraction of the number of reducible sites seen in the Mössbauer spectrum will be investigated further with improved *in situ* experiments.

Conclusions

Comparison of the chemisorption and catalysis of $H_2 + CO_2 \rightarrow CO + H_2O$ over Eu_2O_3 versus europium highly dispersed on Al_2O_3 and SiO_2 has revealed some interesting differences. While both irreversible and reversible chemisorption of CO_2 was observed on Eu_2O_3 at 500°C, only reversible CO_2 chemisorption was seen on highly dispersed Eu under the same conditions. In kinetic measurements at CO_2 partial pressures 0.05–0.30 atm, the rate of the reverse of the water–gas shift reaction over Eu_2O_3 showed a sharp maximum as a function of P_{CO_2} while the rate was nearly zero order in CO_2 over supported europium. The kinetic data for Eu_2O_3 are well described by a regenerative oxidation–reduction sequence including poisoning by strong CO_2 chemisorption. Over supported Eu, the rates were also consistent with the regenerative kinetic sequence but with no CO_2 poisoning. Furthermore, these rates showed a good correlation with the amount of Eu^{2+} observed in a room temperature Mössbauer spectrum after reduction for 6 hr in H_2 at 500°C.

From the kinetic analysis, the ratio of the effective surface reduction rate constant to the effective surface oxidation rate constant was close to one for Eu_2O_3 but less than one-tenth for supported Eu. This result leads to the conclusion that when Eu^{3+} is dispersed on Al_2O_3 or SiO_2 its rate of surface reduction is lower, with respect to oxidation, than that for Eu_2O_3. In addition, dispersed Eu chemisorbs CO_2 in a manner more similar to that of the support than to that of bulk Eu_2O_3. These changes in surface chemistry are taken as a result of the strong support interactions indicated by the effective Debye temperatures obtained from Mössbauer spectra. This type of interaction may be discussed in terms of a surface compound or the local environment of the cation of interest. It suggests, as has already been confirmed in a number of other systems (e.g., *6*, *23*) that significant support influence on catalyst chemistry should be expected when *cations* are highly dispersed on oxides.

Acknowledgments

This work has been supported by NSF institutional grant GU-3282 to Yale University and grants from the Chevron Research Company. Acknowledgment is also made to the donors of the Petroleum Research Fund, administered by the American Chemical Society, for partial support of this work. We also thank Texaco Inc. for a graduate fellowship to PNR during part of the

work, S. B. Weiner for the use of his fitting program, and J. C. Vartuli for helpful discussions during preparation of this manuscript.

References

1. Boreskov, G. K., *Kinet. Katal.* **11**, 374 (1970).
2. Boreskov, G. K., Dzisyak, A. P., and Kasatkina, L. A., *Kinet. Katal.* **4**, 388 (1963).
3. Sazanov, V. A., Popovskii, V. V., and Boreskov, G. K., *Kinet. Katal.* **9**, 307 (1968).
4. Antoshin, G. V., Minachev, K. M., and Dimitriev, R. V., *Kinet. Katal.* **9**, 816 (1968).
5. Ross, P. N., Jr., and Delgass, W. N., "Catalysis" (J. W. Hightower, Ed.), Vol. 1, p. 597. North Holland, New York, 1973.
6. Selwood, P. W., "Advances in Catalysis," Vol. 3, p. 27. Academic Press, New York, 1951.
7. Ross, P. N. Jr., Ph.D. Thesis, Yale University, 1973.
8. Minter, C. C., *J. Phys. Chem.* **72**, 1924 (1968).
9. Margulies, S., and Ehrman, J. R., *Nuclear Instrum. and Methods* **12**, 131 (1961).
10. Shirley, D. A., Kaplan, M., Grant, R. W., Keller, D. A., *Phys. Rev.* **127**, 2097 (1962).
11. Amer. Inst. Physics Handbook, 2nd Edition, p. 4–62 (1964).
12. Calculated from low temperature heat capacity data in *International Critical Tables*, Vol. 5, p. 98.
13. Visscher, W. M., *Phys. Rev.* **129**, 28 (1963).
14. Burton, J. W., Frauenfelder, H., and Godwin, R. P., *Applications of Mössbauer Effect in Chemistry*, Tech. Rept. Ser. **50**, Int. AEC, Vienna (1966), pp. 73–87.
15. Gerth, G., Kienle, P., and Luchner, K., *Physics Letters* **27A**, 557 (1968).
16. Samuel, E. A., Ph.D. Thesis, Yale University, 1973.
17. Barret, M. F., and Barry, T. I., *J. Inorg. Nuc. Chem.* **27**, 1483 (1965).
18. Artamov, E. V., and Sazanov, L. A., *Kinet. Katal.* **12**, 961 (1971).
19. Mamedov, E. A., Popovskii, V. V., and Boreskov, G. K., *Kinet. Katal.* **10**, 852 (1969).
20. Makishima, S., Yoneda, Y., and Saito, Y., *Proc. 2nd Int. Cong. on Catalysis*, Vol. 1, Editions Technip, Paris (1960), p. 617.
21. Weiner, S., Ph.D. Thesis, Yale University, 1972.
22. Boudart, M., Mears, D. E., and Vannice, M. A., "Congres International de Chimie Industrielle," *Ind. Chim. Belge*, Special Issue **36**, Part I, 281 (1967).
23. Cimino, A., Pepe, F., and Schiavello, N., "Catalysis" (J. W. Hightower, Ed.), Vol. 1, p. 125. North Holland, New York, 1973.